Kinetic Resolution of a Conformational Transition and the ATP Hydrolysis Step Using Relaxation Methods with a *Dictyostelium* Myosin II Mutant Containing a Single Tryptophan Residue[†]

András Málnási-Csizmadia,[‡] David S. Pearson,[§] Mihály Kovács,[‡,||] Robert J. Woolley,[‡] Michael A. Geeves,[§] and Clive R. Bagshaw*,[‡]

Department of Biochemistry, University of Leicester, Leicester LE1 7RH, U.K., Research School of Biosciences, University of Kent, Canterbury, Kent CT2 7NJ, U.K., and Department of Biochemistry, Eötvös University, H-1088 Budapest, Hungary

ABSTRACT: The fluorescence emission intensity from a conserved tryptophan residue (W501) located in the relay loop (F466 to L516) of the *Dicytostelium discoideum* myosin II motor domain is sensitive to ATP binding and hydrolysis. The initial binding process is accompanied by a small quench in fluorescence, and this is followed by a large enhancement that appears coincident with the hydrolysis step. Using temperature and pressure jump methods, we show that the enhancement process is kinetically distinct from but coupled to the hydrolysis step. The fluorescence enhancement corresponds to the open−closed transition ($k_{obs} \approx 1000$ s^{-1} at 20 °C). From the overall steady-state fluorescence signal and the presence or absence of a relaxation transient, we conclude that the ADP state is largely in the open state, while the ADP·AlF$_4$ state is largely closed. At 20 °C the open−closed equilibria for the AMP·PNP and ADP·BeF$_x$ complexes are close to unity and are readily perturbed by temperature and pressure. In the case of ATP, the equilibrium of this step slightly favors the open state, but coupling to the subsequent hydrolysis step gives rise to a predominantly closed state in the steady state. Pressure jump during steady-state ATP turnover reveals the distinct transients for the rapid open−closed transition and the slower hydrolysis step.

Tryptophan fluorescence has been used widely as a probe for the different conformational states of myosin during its interaction with ATP (*1−6*). In the case of vertebrate skeletal muscle myosin, an enhancement in tryptophan emission intensity is observed on binding nucleotide and a further change is seen coincident with the hydrolysis step. The latter property appears to be a general feature of myosin II isoforms. Chemical probe (*7−9*) and site-directed mutagenesis studies (*10−13*) have identified the tryptophan residue responsible for the enhancement associated with hydrolysis as a conserved residue located at the end of the relay loop [chicken skeletal myosin W510; smooth myosin W512; *Dictyostelium discoideum* (Dd)[1] myosin W501]. Indeed, this residue is conserved in most myosin classes, including I, V, VII, VIII, IX, X, XI, and XIII, making it an ideal natural probe. The relay loop tryptophan residue is some 3.5 nm from the ATPase site and indicates that a conformational transition, associated with hydrolysis, is propagated through a substantial part of the motor domain. The nature of this transition has been clarified by X-ray crystallographic studies

which show that as the switch 2 loop at the ATPase site moves toward the γ-phosphate of ATP (the so-called "open−closed" transition), it allows the converter region to roll around the relay helix bearing the sensitive tryptophan residue (*14−19*). Events at the active site are transmitted to the light chain binding domain (the putative lever arm) via the converter domain and control the angle at which the light chain binding domain extends relative to the motor domain. The active site open−closed transition thus equates with the down−up disposition of the light chain binding domain. Reversal of this process, while the motor domain is attached to actin, could constitute the power stroke during the cross-bridge cycle.

From detailed consideration of the crystal structure it has been proposed that the switch 2 loop must move prior to hydrolysis to bring the catalytic residues into place (*18, 19*). Thus, in principle, the open−closed transition and actual hydrolysis step are distinct processes, although whether they are resolvable in practice depends on the kinetics of these reactions. If hydrolysis is fast relative to the open−closed transition, then the steps will appear coincident. If hydrolysis is slower, then there is a possibility of kinetic resolution. Furthermore, if the steps are distinct processes, then there is a possibility of their decoupling using mutants or nucleotide analogues; i.e., the open−closed transition could occur without hydrolysis. Evidence suggestive of separate steps came from mutagenesis of the switch 2 region which produced some constructs that gave enhanced fluorescence

without hydrolysis (*20, 21*). In addition, we showed that, at elevated temperatures, the nonhydrolyzable analogue AMP·PNP could induce a closed state, as indicated by the fluorescence of W501 in a single tryptophan construct (*13*). Consequently, the generally accepted ATPase mechanism has been extended to include an additional intermediate (M*·ATP) corresponding to a closed unhydrolyzed ATP state (*13, 18*) (eq 1). Using a Dd motor domain construct, W501+,

$$
\begin{array}{c}
M + ATP \underset{}{\overset{1}{\rightleftharpoons}} M.ATP \overset{2}{\underset{}{\rightleftharpoons}} M^{\dagger}.ATP \overset{3a}{\underset{}{\rightleftharpoons}} M^*.ATP \overset{3b}{\underset{}{\rightleftharpoons}} M^*.ADP.Pi \\
\quad\quad\quad\quad\quad\quad\quad\quad\quad\quad\quad\quad\quad\quad\quad\quad\quad\quad\quad\quad\quad \updownarrow 4 \\
M + ADP \overset{7}{\underset{}{\rightleftharpoons}} M.ADP \overset{6}{\underset{}{\rightleftharpoons}} M^{\dagger}.ADP + Pi \overset{5}{\underset{}{\rightleftharpoons}} M^{\dagger}.ADP.Pi \quad (1)
\end{array}
$$
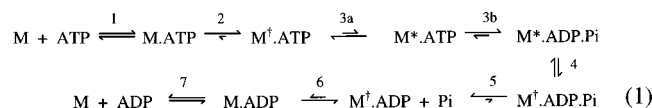
containing a single tryptophan residue, we showed that this residue responds with a 10−15% quench in fluorescence on nucleotide binding and a 50−80% enhancement on hydrolysis of ATP (*13, 22*). The finding of a quench on binding shows that the apo and open nucleotide-bound states have distinct conformations that may be related to a third crystal state characterized using a scallop myosin subfragment (*17*). An enhancement in fluorescence on nucleotide binding to vertebrate skeletal myosins may reflect contributions from other nonconserved tryptophan residues (*18*).

Demonstrating that the open−closed transition induced by ATP itself is distinct from hydrolysis using rapid mixing methods is challenging. In principle, the scheme shown in eq 1 might reveal a succession of phases on mixing ATP with apo Dd W501+: a very rapid quench associated with $M^{\dagger}$·ATP formation (k_2) and a small rapid enhancement associated with limited M*·ATP formation ($k_{3a} + k_{-3a}$), followed by a slower enhancement as hydrolysis to M*·ADP·P_i pulls the equilibrium toward the closed state ($K_{3a}k_{3b} + k_{-3b}$). However, if the $M^{\dagger}$·ATP $\leftrightarrow$ M*·ATP transition (step 3a) is as fast as or faster than step 2, then these species will be formed with practically the same time course, and whether an initial quench or enhancement is seen will depend on the equilibrium constant (K_{3a}) between them. The absence of either a significant initial quench or burst in fluorescence when ATP interacts with the W501+ motor domain could be taken as evidence of limited M*·ATP formation that cancels the quench expected for $M^{\dagger}$·ATP, and thus K_{3a} is in the region of 0.1−0.5 at 20 °C (*13*). Here we provided support for this proposal using perturbation methods to dissect kinetically the two steps, 3a and 3b, associated with hydrolysis. Thus these data support the hydrolysis mechanism deduced from the crystal structures (*18, 19*).

Rapid mixing techniques are limited in their ability to resolve a fast step that follows a slower one. Perturbation methods (temperature and pressure jump) may overcome this limitation provided that the rapid step is freely reversible (as proposed for step 3a) and it is susceptible to the perturbant. Perturbation methods may also reveal transients that are lost in the dead time of rapid mixing techniques because they have better time resolution. Current data indicate that step 2 in the nucleotide binding mechanism lies far to the right, especially for the interaction with ATP, and thus it would not show a significant transient on perturbation (even though the rate constant k_{-2} probably has a high temperature dependence). On the other hand, hydrolysis and the open−closed transition appear more freely reversible and are temperature sensitive (*13*). Temperature jump would

therefore seem a good technique to resolve step 3a from step 2.

Recently, Jahn et al. (*23*) have carried out temperature jump studies on vertebrate skeletal muscle myosin fragments and have observed rapid changes in tryptophan fluorescence that they interpret as evidence for a loose coupling between the myosin conformation and the hydrolysis reaction. We extend these measurements using the Dd single tryptophan mutant, W501+, with the advantage that the origin of the signal is limited to a single known site and the background signal from nonresponding tryptophan residues is eliminated.

We also demonstrate the advantages of the pressure jump method for revealing relaxation kinetics that proved particularly significant when using microvolume cells. Pressure jump measurements have several advantages over temperature jump perturbations (*24*). High repetition rates are possible, allowing data collection with improved signal-to-noise ratios because there is no equivalent of a cooling phase. Pressure perturbation by a piezo crystal is particularly efficient in allowing repetition at up to 12.5 Hz (*25*), and jumps can be recorded in both directions. In addition, the reaction can be followed on long time scales if desired because the pressure remains constant after the jump. Samples do not require high ionic strength, as is needed for efficient joule heating in temperature jump. Furthermore, the intrinsic fluorescence of tryptophan shows little pressure sensitivity over the range used for perturbation kinetics, so there is no transient associated with the jump itself, in contrast to the effect of a temperature change.

MATERIALS AND METHODS

Materials. The Dd myosin motor domain (W501+) containing a single tryptophan residue W501 was prepared as described previously by mutagenizing the remaining native tryptophan residues to phenylalanine (*13*). W501+ is thus a triple mutant with the substitutions W36F, W432F, and W584F. The mutagenized insert was subcloned into the Dd pDXA-3H expression vector (*26*) that resulted in a construct with a modified N terminus *MDGTED*P... in place of MNP... and a His-tagged C terminus ...R*LGSTRDALH*$_8$, where R761 is the last native residue in the wild-type sequence.

Nucleotides were purchased from Sigma Chemical Co. (Poole, U.K.). The M·ADP·BeF$_x$ complex was prepared by incubation of 5−40 μM W501+, 50 μM ADP, 3 mM NaF, and 50 μM BeCl$_2$ for 30 min. The M·ADP·AlF$_4$ complex was made similarly but with 50 μM AlCl$_3$ and incubation for at least 60 min.

Fluorescence Measurements. Steady-state fluorescence time courses were measured with an SLM 48000 spectro-fluorometer with a 450 W xenon lamp using a 5 mm path length cell. Tryptophan was excited at 295 nm and 1 nm bandwidth to minimize photobleaching and excitation of tyrosine and to reduce inner filter effects arising from high nucleotide concentrations. The temperature dependence of the fluorescence was measured by cooling the sample (from 25 to 5 °C) over a period of 15 min with circulating water while simultaneously recording the fluorescence and temperature of the cell contents using a probe thermometer (RS158-430, Corby, U.K.).

Transient fluorescence measurements were carried out using an Applied Photophysics SX18MV stopped-flow fluo-

rometer with a WG320 cutoff emission filter in combination with a UG11 filter to block visible stray light. Reactions were studied in a buffer comprising 40 mM NaCl, 20 mM TES, and 1 mM MgCl$_2$ at pH 7.5, and the reagent concentrations stated refer to the reaction chamber unless otherwise stated. Data were normally collected on a logarithmic time base to ensure that there were a significant number of data points for all phases of multistep reactions. The dead time of the apparatus was determined as 1.5 ms from the reaction of NATA with *N*-bromosuccinimide (*27*).

Temperature Jump Instrument. Temperature jump experiments were carried out using the TJ-64 System (Hi-Tech Scientific, Salisbury, U.K.). The sample was excited at 297 nm light using a 75 W Hg−Xe lamp (Hamamatsu Photonics, Enfield, U.K.) and a 297FS10-25 interference filter (Andover Corp., L.O.T. Oriel Group, Leatherhead, U.K.). The emitted light was collected through UG11 band-pass and 320 nm cutoff filters. The temperature jump was achieved with a 10 kV discharge through the cell (100 μL volume, 3 mm optical path length) that gave an approximately 5 °C temperature increase in less than 5 μs at high ionic strength (>0.5 M). However, with the lower ionic strength conditions used for experiments, the heating time was approximately 50 μs. The cooling half-time was approximately 3 s, but it was not a single exponential event. Generally, a 150 s interval was left between temperature jumps. Reactions were studied in a buffer comprising 60 mM NaCl, 20 mM TES, and 1 mM MgCl$_2$ at pH 7.5 at an initial temperature of 16 °C. This was the lowest ionic strength buffer that permitted satisfactory electrical and thermal conduction.

Pressure Jump Instrument. The pressure jump apparatus is based on the original design of Clegg and Maxfield (*25*) except that the internal volume was reduced to 50 μL and the solution was exchanged via two low-volume pressure valves, making the system much simpler to operate. The sample was held in an optical chamber consisting of a sapphire ring (2 mm inner diameter, 5 mm outer diameter, 5 mm height). The ends of the chamber were closed by a pressure sensor (Kistler 601A) on one end and a piston attached to a piezo-electric translator (Physik Instrumente P245.30) at the other. The sample was isolated from the piston by a thin membrane (0.003 in. thick Kaptan V, Du Pont, Kensulat Ltd., U.K.). A step voltage of up to 1 kV was used to stimulate the translator, developing pressure changes of 80 bar in approximately 80 μs for both increasing and decreasing pressure. Fluorescence was excited at 297 nm using light from a 100 W Hg−Xe lamp, which was passed through a monochromator having slit widths of 2.5 nm. Emitted light was selected through a WG320 cutoff filter before being detected at the photomultiplier. Pressure jumps and data collection were automated, allowing repeat jumps at a rate up to 12.5 s^{-1}.

RESULTS

Temperature Dependence of Fluorescence Emission. The fluorescence emission intensity of tryptophan and its derivatives is inherently temperature sensitive owing to the effect on the rate of nonradiative decay processes that reduce the lifetime of the excited state. In practice, the signal typically decreases by about 1% per 1 °C increase in temperature. If a protein is present in two conformational states in which
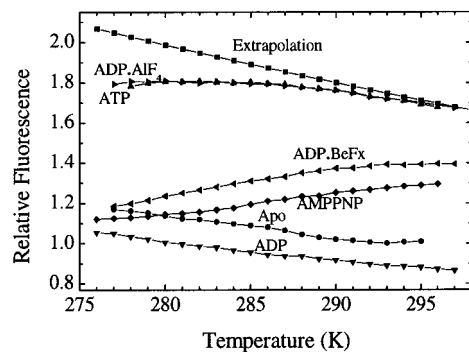

FIGURE 1: Temperature dependence of the intrinsic fluorescence of W501+ in the absence and presence of different nucleotides. Tryptophan was excited at 295 nm, and the emission was detected at 340 nm. 1 mM ATP, 650 μM ADP, or 200 μM AMP·PNP was added to 9 μM W501+ motor domain in 40 mM NaCl, 20 mM TES, 2 mM MgCl$_2$, and 0.5 mM β-mercaptoethanol at pH 7.5. The ADP·AlF$_4$ and ADP·BeF$_x$ complexes were made, and the temperature was ramped between 297 and 277 K as described in the Materials and Methods section. The extrapolated line is based on a slope of −1% fluorescence change per degree from the 298 K point and was used as a reference for the closed state for calculations in Table 1.

the tryptophan emission signal differs, then the observed temperature dependence of the tryptophan emission intensity will reflect both the temperature dependence of the equilibrium between the states and the underlying inherent temperature dependence of tryptophan emission. Figure 1 shows the temperature dependence of the tryptophan emission intensity of the W501+ motor domain in the absence and presence of nucleotides. The data were normalized to the value for the apo W501+ at 20 °C. The temperature dependence of the apo W501+ protein closely paralleled that of NATA in ethanol solvent and was thus dominated by the inherent sensitivity of tryptophan. Over the range 5−20 °C the fluorescence decrease was approximately linear with a slope of about −1% per °C. This finding indicates the existence of either one dominant conformational state or multiple conformational states whose equilibria are temperature insensitive and/or have similar environments for the W501 residue. Operationally, the apo state may therefore be treated as a single conformational state in the present studies. Multiple microstates in rapid equilibrium, possibly corresponding to tryptophan rotamers, were revealed in time-resolved fluorescence studies (*22*). Addition of saturating ADP to the W501+ motor domain caused a 12% quench in fluorescence, as noted previously (*13*), but the slope of the temperature profile remained similar to the apo state. This result is consistent with the formation of a new dominant "single" conformational state. Again, microstates are apparent in time-resolved measurements (*22*), but the proportions of these do not seem particularly temperature sensitive.

Addition of ATP to W501+ gives about an 80% fluorescent enhancement at temperatures above 15 °C (Figure 1). However, the temperature profile deviates from the approximately linear dependences observed in the apo and ADP-bound states. This suggests that a second conformation makes a small but significant contribution to the steady-state complex particularly at low temperatures. Care was taken in these studies to ensure that the ATP was not exhausted during the experiment. The analysis of the ATP data is considered further below. The temperature profile of the ADP·AlF$_4$ complex closely follows that of the steady-state

Table 1: Equilibrium Constant and Related Parameters for the Open−Closed Transition Based on the Steady-State/Equilibrium Tryptophan Fluorescence Intensity of the W501+ Motor Domain[a]

temp (°C)	$^{app}K_{oc}$			ΔG_o (kJ/mol)			ΔH_o (kJ/mol)		
	AMP·PNP	BeF$_x$	ATP	AMP·PNP	BeF$_x$	ATP	AMP·PNP	BeF$_x$	ATP
5	0.11	0.20	3	5.2	3.8	−2.6	132	133	117
10	0.25	0.46	7	3.3	1.8	−4.4	96	94	92
15	0.49	0.85	14	1.7	0.38	−6.4	68	78	96
20	0.82	1.43	32	0.49	−0.87	−8.4	66	60	114
23	1.06	1.74	45	−0.14	−1.4	−9.4	60	58	82

[a] Values of $^{app}K_{oc}$ were based on the fluorescence intensities in Figure 1 using the ADP data and extrapolated data as measures of fluorescence of the open (F_o) and closed (F_c) states, respectively: thus $^{app}K_{oc} = (F_c - F)/(F - F_o)$, $\Delta G_o = -RT \ln K_{oc}$, and ΔH_o was calculated from the slope of the van't Hoff plot (ln $^{app}K_{oc}$ against $1/T$). Note, in the case of ATP, that the open−closed transition is coupled to hydrolysis such that $^{app}K_{oc} = K_{3a}(1 + K_{3b})$ in eq 1, where the value of $K_{3a} < 1$ and comparable to $^{app}K_{oc}$ in the presence of AMP·PNP.

complex observed during ATP turnover. The ADP·Vi complex also showed a similar profile, but the emission intensity was reduced by about 6% relative to that for ADP·AlF$_4$, probably due to the absorbance of the Vi. The most striking change in the observed temperature profile was obtained in the presence of AMP·PNP or ADP·BeF$_x$. These complexes showed intermediate fluorescence intensities but the opposite slope compared to the apoprotein; i.e., fluorescence increased with increasing temperature. Previously, we argued (13) that the quench in W501+ fluorescence with ADP (M†·ADP) corresponded with the open state identified by crystallography (18), while the enhancement seen with ATP at high temperature was predominantly the closed state (M*·ADP·P$_i$). On this basis it appears that AMP·PNP and ADP·BeF$_x$ induce a mixture of the two states in comparable proportions, and thus temperature jump measurements should reveal the time course of the open−closed transition. From the intensity of the fluorescence relative to that in the presence of ADP and the ADP·AlF$_4$ complex, the apparent equilibrium constant for the open−closed transition, $^{app}K_{oc}$, can be estimated at each temperature (Table 1). Uncertainty exists as to the fluorescence value for the 100% closed state at low temperatures, but an estimate can be made by linear extrapolation from data at higher temperatures with a slope of −1% per °C. Previous estimates of the value of $^{app}K_{oc}$ (equivalent to K_{3a} in eq 1) for AMP·PNP bound to W501+ using amplitudes deduced from stopped-flow traces (13) showed the same high temperature dependence but slightly lower absolute values compared with those determined from the steady-state data in Table 1.

The situation with ATP during steady-state turnover is more complicated because the open−closed transition is coupled to the hydrolysis step. In terms of eq 1, $^{app}K_{oc} = K_{3a}(1 + K_{3b})$, while the equilibrium for the hydrolysis step, as determined from the amplitude of the phosphate burst, $^{app}K_h = K_{3b}K_{3a}/(1 + K_{3a})$ where at ambient temperatures $K_{3a} < 1$ and $K_{3b} > 1$. In effect, the hydrolysis step pulls the conformation toward the closed state, while the open−closed transition tends to pull the hydrolysis equilibrium back toward the M†·ATP state, making hydrolysis appear more reversible. Limits can be placed on the values of K_{3a} and K_{3b} on the basis of the amplitudes of stopped-flow and pressure jump transients described below and quench flow

data (13). From analysis of Figure 1 an estimate of $^{app}K_{oc}$ can be made at each temperature (Table 1) and shows that the closed state predominates throughout during steady-state ATP hydrolysis. These estimates, when interpreted alongside other results, appear to provide an upper limit for $^{app}K_{oc}$. Systematic errors arise from knowledge of the fluorescence for the fully closed state and also possibly because a small but variable slow phase in ATP-induced W501 fluorescence enhancement (k_{obs} around 0.2 s^{-1}) of unknown origin may give a slight overestimate of the fluorescence level recorded during steady-state hydrolysis (13). Furthermore, the calculation of $^{app}K_{oc}$ has a progressively larger error as the observed fluorescence intensity approaches the limits of the fully open or closed state (i.e., when $^{app}K_{oc} < 0.1$ or $^{app}K_{oc} > 10$).

As outlined in the introduction, it is not possible to resolve the separate contributions of M†·ATP and M*·ATP at 20 °C by rapid mixing methods although an estimate can be made for the magnitude of K_{3a} to account for the absence of a transient in fluorescence emission that precedes the hydrolysis step. A possible small quench was observed in previous records (13), but this was difficult to distinguish from flow artifacts at 20 °C. This observation suggests that the concentrations of M†·ATP and M*·ATP in the early phase of the reaction, weighted by their relative fluorescence emission (0.85:1.5), are balanced to give an observed fluorescence close to 1 (i.e., equivalent to the apo W510+ level) and thus $K_{3a} \approx 0.3$. A quench or burst phase should be detectable if K_{3a} is outside the limits $0.2 < K_{3a} < 0.5$. Note that the observed fluorescence changes are instrument-dependent and generally smaller when a band-pass emission filter is used, as in the stopped-flow apparatus (13, 22). At low temperatures the binding process was slowed to allow better detection within the dead time, and the equilibria appeared perturbed to favor the M†·ATP state (13). Stopped-flow studies were therefore carried out at lower temperatures to confirm this trend (Figure 2a). A clear initial quench phase was seen at 2 °C, indicating that, under these conditions, either $k_2 > k_{3a} + k_{-3a}$ and/or $K_{3a} \leq 0.2$ so that the weighted fluorescence from M†·ATP + M*·ATP was less than that from the apo state. The rate constant for the quench provides a value of $k_2 = 130$ s^{-1}. Independent estimates of k_2 and k_{-3a} (see below; Table 2) indicate that they are temperature dependent but of similar magnitude at all temperatures, and thus a small shift in the equilibrium constant K_{3a} appears to be the more significant process in producing an observable quench at low temperatures. At higher temperatures, M*ATP makes a greater contribution that nullifies the quench, but not so great as to give a detectable burst in fluorescence ahead of the hydrolysis step. These stopped-flow studies (Figure 2b) also reveal a strong temperature dependence of the observed rate constant of the enhancement phase associated with the hydrolysis step [$k_{obs} = (K_{3a}k_{3b}/(1 + K_{3a})) + k_{-3b}$ on the basis of eq 1]. This dependence reflects the rate constants for step 3b directly, as well as the shift in the equilibrium constant K_{3a} (Table 2). Knowing that $K_{3a} < 1$ and $^{app}K_{oc} > 1$ requires $K_{3b} \gg 1$, and thus $^{app}K_{oc} \approx K_{3a}K_{3b}$ for ATP throughout the temperature range studied. In analysis in terms of $^{app}K_{oc} = K_{3a}(1 + K_{3b})$, the contribution of M†·ADP is ignored, but this species makes a negligible contribution (around 1%) at 20 °C on the basis of the kinetics of its dissociation (13). We have also determined the dissociation rate of ADP from M†·ADP at low temperatures and shown
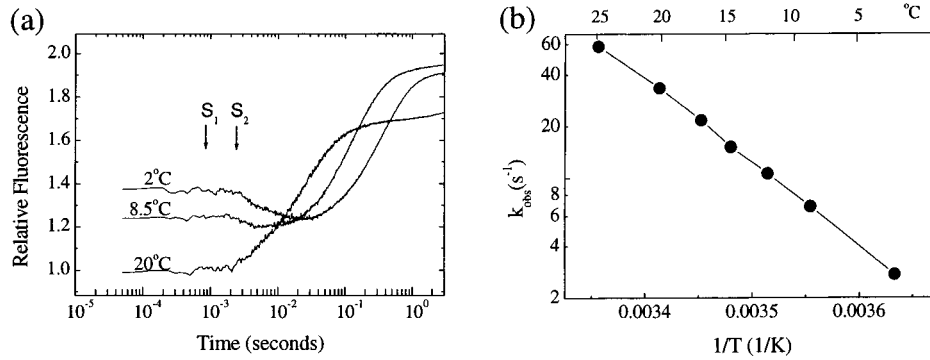
FIGURE 2: Reaction of W501+ with ATP at different temperatures in the stopped-flow apparatus. (a) 2 μM W501+ was rapidly mixed with 250 μM ATP (reaction chamber concentrations) at 2, 8.5, and 20 °C, and the intrinsic fluorescence was followed. The excitation wavelength was 295 nm, and the emission signal was selected with a combination of 320 nm cutoff and UG11 filters. The buffer was as described in Figure 1. The reaction was recorded on a log time base with a short pretrigger. The arrow labeled S_1 corresponds to the calculated start of the reaction and S_2 to the stop of the ram monitored by a potentiometer. (b) Temperature dependence of the rate constant of the dominant enhancement phase (apparent hydrolysis rate) observed in stopped-flow records. Records, as exemplified in (a), were fit to double or triple exponentials. The latter was required to fit the quench phase that was only resolved below 12 °C. All reactions contained a minor slow phase of enhancement that amounted to 10−20% of the reaction (*13*). The slope of the graph yielded an apparent activation energy $E_a = 11$ kJ mol^{-1}, but this involves at least two temperature-dependent steps: $K_{3a}k_{3b} + k_{-3b}$ (eq 1 and Table 2).

Table 2: Rate and Equilibrium Constants for the Open−Closed Transition and ATP Hydrolysis Steps for the W501+ Motor Domain Based on Steady-State Fluorescence, Stopped-Flow, and Pressure Jump Transients

nucleotide	temp (°C)	$^{app}K_{oc}$ (fluor)^a	$^{app}K_{oc}$ (PJ)^b	K_{3a} (SF)^c	k_{3a} (s^{-1})^d	k_{-3a} (s^{-1})^d	K_{3b} (fluor)^e	K_{3b} (PJ)^f	k_{3b} (s^{-1})^g	k_{-3b} (s^{-1})^h
ATP	5	3	1.9	0.2	54	270	14	8	17−20	1.2−2.5
	15	14	4.6	0.3	150	490	45	14	53−63	1.2−4.5
	20	32	5.7	0.4	350	870	79	13	90−110	1.1−8.5
ADP·BeF$_x$	5	0.20	0.43		30	150				
	10	0.46	0.55		70	150				
	13	1.32	1.0		180	140				
	20	1.43	2.3		250	170				
	25	1.74	2.6		370	210				
AMP·PNP	5	0.11	<0.1		nd^i	nd^i				
	10	0.25	0.16		92	370				
	15	0.49	0.32		210	420				
	20	0.82	1		460	570				
	25	1.06	1		1000	950				

^{a} From steady-state fluorescence level (Table 1). ^{b} From pressure jump (PJ) amplitude ($K = 1$ when ΔF is maximal). ^{c} From stopped-flow (SF) fluorescence burst/quench transient (cf. Figure 2a) and pressure jump analysis (see text). ^{d} From pressure jump kinetics, $k_{obs} = k_{3a} + k_{-3a}$ and $K_{3a} = k_{3a}/k_{-3a}$. For ADP·BeF$_x$ and AMP·PMP, $K_{3a} \equiv ^{app}K_{oc}$ and was taken from footnote a. ^{e} Calculated from steady-state fluorescence $^{app}K_{oc}$ with $K_{3b} = (^{app}K_{oc}/K_{3a}) - 1$. ^{f} Calculated pressure jump $^{app}K_{oc}$ with $K_{3b} = (^{app}K_{oc}/K_{3a}) - 1$. ^{g} From stopped-flow transient k_{obs} (Figure 2b); $k_{3b} = k_{obs}/[(K_{3a}/(1 + K_{3a})) + 1/K_{3b}]$. The range is calculated for the two estimates of K_{3b} (footnotes e and f). ^{h} From $k_{-3b} = k_{3b}/K_{3b}$ using ranges in footnotes e−g. ^{i} nd: not determined because amplitude was too small.

that it remains significantly faster (>20 times) than the steady-state rate and thus M†·ADP makes ≤5% contribution.

Temperature Jump Measurements. Figure 3 shows temperature jump profiles for NATA and the W501+ motor domain in the apo form and in the presence of AMP·PNP and ADP·BeF$_x$. In these measurements the NaCl was increased to 60 mM to aid electrical and thermal conduction through the cell. The temperature jump profiles of NATA and apo W501+ could be superposed and reflect the rapid heating and slow cooling of the sample (the former is limited by the instrument time constant in the records shown in Figure 3a). The amplitudes of the transient decrease in the fluorescence signal ($\Delta F = -12\%$) indicate that the temperature jump was of the order of 10 °C (cf. Figure 1 for the apo W501+ profile). The profiles in the presence of AMP· PNP and ADP·BeF$_x$ were markedly different from that of apo W501+ in showing an additional rising phase on the millisecond time scale (Figure 3b), indicative of reequilibration of conformational states. Fits to this phase yielded

rate constants of the order of 1000 s^{-1} that we assign to the open−closed transition ($k_{obs} = k_{3a} + k_{-3a}$; see Discussion). These data appear similar to those of Jahn et al. (*23*) for vertebrate skeletal myosin fragments. It is pertinent to note that the temperature jump transient observed for the M·ADP· BeF$_x$ complex (Figure 3b) is more than 3 orders of magnitude faster than the maximum rate of formation of this complex on addition of BeF$_x$ to M†·ADP (0.15 s^{-1} at 20 °C; data not shown).

While the microcell (0.1 mL) of the Hi-Tech TJ-64 temperature jump apparatus conserves sample, the elevated temperature is only briefly maintained. The half-time for cooling was approximately 3 s, but the profile was not a simple exponential function, and correction of the baseline to extract parameters for any process whose amplitude was <1/10 the intrinsic fluorescence change and whose rate constant was <50 s^{-1} was difficult. On the basis of the amplitude of transient observed in the presence of AMP· PNP and ADP·BeF$_x$ (about +10% after correction for apparatus time constant; Figure 3b) compared with the
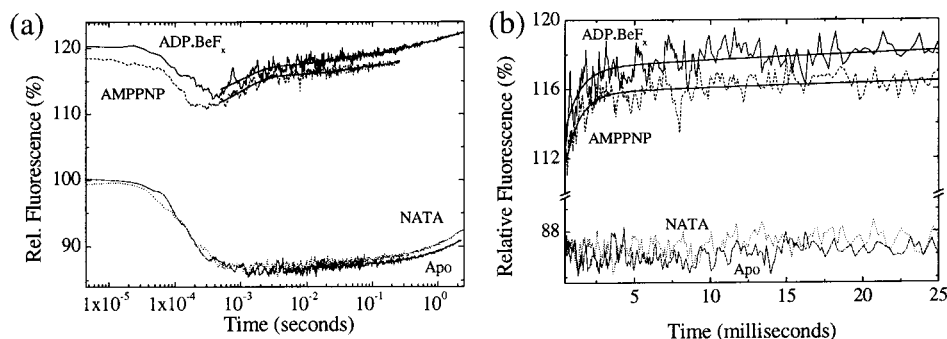
FIGURE 3: Temperature jump records of NATA and W501+ in the absence and presence of AMP·PNP and ADP·BeF$_x$. Tryptophan fluorescence was followed after an approximately 10 °C temperature jump from a starting temperature of 16 °C. 30 μM NATA or 16 μM W501+ was prepared in 60 mM NaCl, 20 mM TES, 2 mM MgCl$_2$, and 0.5 mM β-mercaptoethanol at pH 7.5. W501+ was examined in the apo state and in the presence of 200 μM AMP·PNP or 50 μM ADP·BeF$_x$ (see Materials and Methods section). 100% relative fluorescence represents the emission level of the W501+ in the absence of nucleotide at 16 °C, and 0% is the background signal of the assay buffer. (a) shows reaction records on a log time base and includes the heating and cooling phases. The heating phase was limited by the filter time constant of 100 μs. (b) records on a short linear time base to show transient enhancement of W501+ fluorescence in the presence of AMP·PNP or ADP·BeF$_x$ that is absent in apo W501+ and NATA. Exponential fits yield rate constants of 1025 $\pm$ 65 s^{-1} (AMP·PNP) and 1086 $\pm$ 117 s^{-1} (ADP·BeF$_x$).

overall change expected for a 10 °C rise on a long time scale (Figure 1), any slower transient lost in the cooling phase must have a relatively minor contribution.

Fifty transients were averaged to give the records shown in Figure 3 and took just over 2 h to accumulate. Temperature jump studies were not performed in the presence of ATP because the time needed for cooling between successive jumps (150 s) did not allow a sufficient number of repeats to reduce noise by averaging before the ATP was hydrolyzed.

Pressure Jump Measurements. Perturbation by pressure jump depends on a volume change between the reactants and is particularly sensitive to changes in solvation structure. For small molecule systems, such as pH buffers, temperature and pressure jumps often have differential effects. Thus the pK of amine buffers that show large heats of ionization are preferentially perturbed by temperature, whereas phosphate buffers are more sensitive to pressure (*24*). Global conformational rearrangements in proteins are likely to involve changes in the environment of numerous residues, and thus transitions that show a large temperature dependence often show marked pressure sensitivity as well.

Pressure jumps of 60 bar had no effect on the fluorescence of NATA. Also no pressure-induced transients were detected on any time scale (up to 15 s) for the apo W501+ motor domain (Figure 4a) nor in the presence of ADP (Figure 4b) or ADP·AlF$_4$ (data not shown). However, W501+ in the presence of AMP·PNP or ADP·BeF$_x$ showed fast transients with kinetics similar to those observed by temperature jump (Figure 4c,d). The signal-to-noise ratio was much improved for a comparable sample volume because of the efficient means of signal averaging in the pressure jump method. In all transients recorded the rate constants for the pressure-up and pressure-down traces were similar, and the amplitudes were of equal magnitude but opposite direction, demonstrating that the perturbations were sufficiently small to result in first-order relaxations. Although the amplitudes of the pressure transients were small ($\leq$1% change in fluorescence) and could be defined with limited precision (0.1%), they provide a useful independent check of the magnitude of the equilibrium constants involved. For a single first-order transition, a small shift in the equilibrium constant, $\Delta K/K$, by perturbation produces a maximum change in concentration

between states, $\Delta C/C$ of 0.25 $\Delta K/K$ when $K = 1$. When $K = 0.1$ or 10, the change in concentration is reduced to 33% of this value i.e., $\Delta C/C = 0.08 \Delta K/K$. To be observable in the pressure jump experiments described here, the equilibrium constant of the transition must lie between 0.03 and 30.

On the basis of the similar kinetics in the presence of ADP· BeF$_x$ and AMP·PNP ($k_{obs} \approx 500-1000$ s^{-1} at 20 °C), it is likely the same step is perturbed by both temperature and pressure, i.e., the open–closed transition. In addition to the rapid phase, a minor phase (20% of the total transient amplitude) was detected in the pressure jump with a rate constant of around 1–2 s^{-1}. The amplitude of the fluorescence change for the M·ADP·BeF$_x$ complex was of the order of 1% of the total fluorescence emission for a 60 bar pressure change and showed a broad maximum in the range of 10–15 °C. The latter observation provides independent evidence that $^{app}K_{oc} \approx 1$ at these temperatures. From the relationship $\Delta K/K = -\Delta P \Delta V/RT$ and assuming the open–closed transition is associated with about a 50% enhancement in fluorescence in the pressure jump apparatus, the volume change associated with the open–closed transition is about +40 mL/mol. The amplitudes of the changes in the presence of AMP·PNP were slightly less and increased with increasing temperature to approach a maximum of around 0.6% change in fluorescence above 20 °C. Below 10 °C the transient was too small to be observed. These data are in line with the steady-state fluorescence measurements (Figure 1) that show for AMP·PNP $^{app}K_{oc} < 1$ at temperatures <20 °C. A volume change of +24 mL/mol was calculated in the presence of AMP·PNP at 20 °C and appeared to decrease slightly with temperature, but the small amplitudes observed limit the accuracy of these calculations.

Pressure jumps during the steady-state hydrolysis of ATP revealed multiple components (Figure 4e,f). In particular, a rapid phase was detected (about 1000 s^{-1} at 20 °C) but with about 20% of the amplitude observed with ADP·BeF$_x$. In addition, a significant transient was observed (24 s^{-1}) with a similar time course for the apparent hydrolysis step measured using rapid mixing methods (Figure 2 and ref *13*), as well as an event at 0.27 s^{-1}. At lower temperatures the total amplitude increased, but the ratio of the fast phase
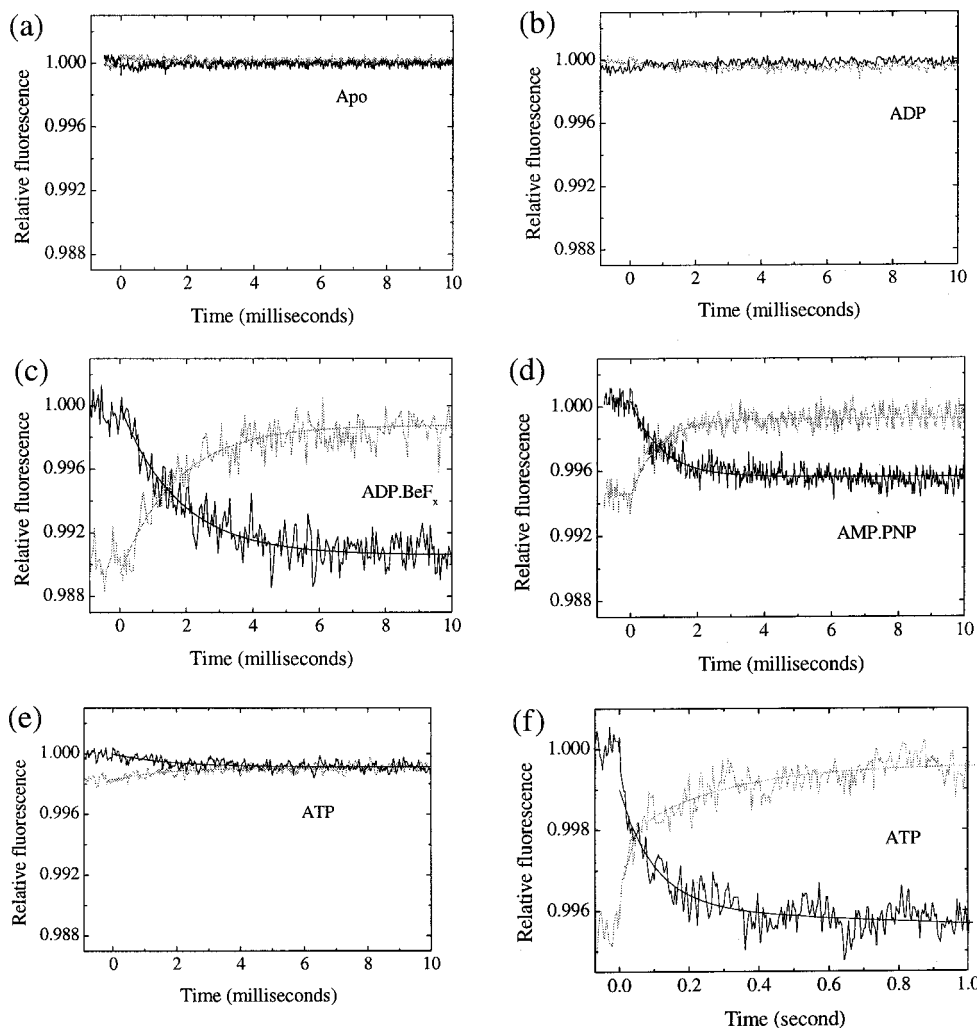
FIGURE 4: Pressure jump records of W501+ in the absence and presence of ATP, ADP·BeF$_x$, AMP·PNP, and ADP. The intrinsic fluorescence change of the W501+ motor domain was measured following pressure jumps between 3 and 60 bar. The black lines represent the pressure-down transients and the gray lines the pressure-up transients. Records were normalized to the starting signal at 3 bar, with zero as the dark signal. The absolute signal was approximately in line with the values shown in Figure 1 but showed some variability between samples and long-term drift. Panels: (a) 40 μM apo W501+, (b) +0.2 mM ADP, (c) +50 μM ADP·BeF$_x$ (see Materials and Methods section), (d) +0.2 mM AMP·PNP, (e and f) +1 mM ATP. Buffer conditions were as in Figure 1 and the experiments performed at 20 °C. In the fast time base records, (a)−(e), data points were collected at 50 μs intervals and the pressure jumps were repeated at a frequency of 12.5 s^{-1}. The data were fitted to single exponential functions in (c)−(e) to give the data plotted in Figure 5. Note that the major transient in the presence of ATP occurs on a slower time scale (f: data points at 4 ms intervals) and required a biphasic fit to yield observed rate constants of 24 and 0.27 s^{-1}.

(200−1000 s^{-1}) to the main phase (2−24 s^{-1}) amplitude remained approximately constant at 1:2 between 5 and 20 °C. At 5 and 20 °C the amplitudes of the total change in the presence of ATP were 90% and 50% the maximum observed change for the M·ADP·BeF$_x$ complex, respectively. These data are consistent with distinct but coupled steps for the open−closed transition and hydrolysis, with the former being rapid and pressure sensitive. Qualitatively, the data are in agreement with the results in Table 1 in requiring the overall $^{app}K_{oc}$ for ATP to approach 1 as the temperature is reduced. If it is assumed that the open−closed transition for ATP (step 3a) has the same volume change as for the M·ADP·BeF$_x$ complex and that the hydrolysis step (3b) is pressure insensitive, then the amplitudes of the fluorescence changes with ATP can be deconvoluted to yield estimates of K_{3a} and K_{3b}. This analysis gives estimates of K_{3a} of 0.2 and 0.4, K_{3b} of 8 and 13, and $^{app}K_{oc}$ of 1.9 and 5.7 at 5 and 20 °C, respectively. Thus K_{3a} is of similar magnitude to the limits set by the stopped-flow transients, but values of $^{app}K_{oc}$ (and

hence K_{3b}) are lower than expected from the data of Table 1 by 2−5-fold. Given the errors and assumptions in analyzing both sets of data, it is not possible to select the more reliable estimate. Both are within the limits established by quenched-flow data (*13*) on this construct (P$_i$ burst at 20 °C $\geq$0.67 mol/mol; therefore, $^{app}K_h \geq 2$, $K_{3b} \geq 7$, and $^{app}K_{oc} > 3$). From the observed rate constant of the transient (Figure 5) and the estimates of the equilibrium constants of the open−closed transition from the data in Table 1, estimates of k_{3a}, k_{-3a}, k_{3b}, and k_{-3b} were obtained for each nucleotide state (Table 2). The uncertainty in the value of $^{app}K_{oc}$ is reflected mainly in the error in k_{-3b}. The magnitude of k_{-3a} is comparable to that of k_2 for ATP (*13*), and thus the M†·ATP and M*·ATP states remain close to equilibrium during their formation by rapid mixing. It is of interest to note (Table 2) that both of the forward rate constants, k_{3a} and k_{3b}, showed marked temperature sensitivity compared with a lesser dependence of k_{-3a} and k_{-3b}, and this leads to the closed state being favored at high temperatures.
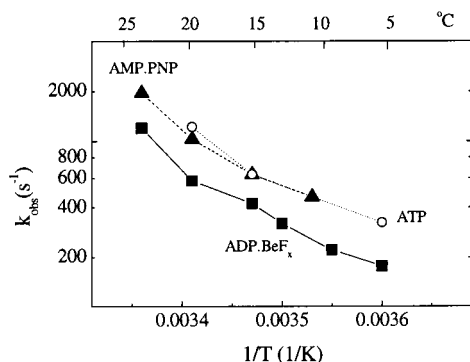
FIGURE 5: Temperature dependence of the observed rate constants of relaxation (fast phase) of W501+ after a pressure jump in the presence of ATP (open circle), AMP·PNP (triangle), and ADP·BeF$_x$ (square). Data were obtained as described in Figure 4. Note that no data were obtained in the presence of ATP at 25 °C or AMP·PNP at 5 °C because the amplitude became too small.

DISCUSSION

Our previous studies (*13*) suggested that the large enhancement in fluorescence emission intensity of W501 in the Dd myosin motor domain, on addition of ATP, is associated with a reaction that is distinct from the ATP hydrolysis step based on the observations (i) that binding of the nonhydrolyzable analogue, AMP·PNP, causes an enhancement in fluorescence at temperatures above 15 °C and (ii) the lack of either a significant rapid quench or rapid enhancement phase on ATP binding at 20 °C prior to the main transient. The latter suggested that a small but significant amount (around 30%) of the M*·ATP species exists transiently whose enhancement cancels the quench attributed to M†·ATP. The latter argument is strengthened by the observation of a quench of fluorescence at low temperatures (Figure 2a), proving the existence of the M†·ATP species under these conditions. In the current work we provide more direct evidence that the fluorescence enhancement step is distinct from the hydrolysis step by their kinetic resolution using perturbation methods. These experiments demonstrate that the open−closed transition is readily reversible and occurs on the submillisecond time scale at temperatures >20 °C. It is of interest that the Dd M·ADP·BeF$_x$ complex has been crystallized in both the open and closed forms, suggesting there is only a small energy barrier between these states (*14, 18*).

We interpret the rapid transients observed by temperature and pressure jump as a result of perturbation of step 3a in eq 1 on the grounds that (i) step 2 would not be significantly perturbed because it is effectively irreversible for ATP and has an equilibrium constant of >100 for other nucleotides and (ii) step 3b cannot occur with AMP·PNP as substrate, yet this nucleotide shows a similar transient to that observed with ATP. There may be some pressure and temperature perturbation of step 3b, but the observed slower phases with ATP (Figure 4f) could arise by a coupled relaxation.

The mechanism of eq 1 fits with the ideas deduced from crystal structures; i.e., once the ATP is bound, switch 2 must move toward the γ-phosphate before hydrolysis can occur (*18, 19*). Movement of the switch 2 loop is coupled to W501 via the relay helix. This allows the converter region to roll around the rest of the motor domain, although it maintains close contact with the relay loop at positions I499−R738

throughout the cycle (*28*). While time-resolved fluorescence and crystallographic studies show that W501 does not reside in a unique conformation for each global conformational state (*22, 29*), a net dequenching of tryptophan fluorescence emission occurs, possibly in part, as a result of increased separation from a conserved basic residue Dd R747 (equivalent to skeletal K768) which is located at the proximal end of the putative lever arm. The kinetic scheme suggests that the motor domain flexes between the open and closed states several times before hydrolysis occurs ($k_{-3a}/k_{3b} \approx 10$ at 20 °C). Hydrolysis is also reversible, but K_{3b} favors the M*·ADP·P$_i$ state. AMP·PNP appears to mimic step 3a with kinetics similar to that of ATP (Figure 5); however, in the absence of hydrolysis, the M†·AMP·PNP state makes a greater contribution to the bound species, and hence a lower net fluorescence enhancement is observed at ambient temperatures. The results here support the proposal of Geeves and Holmes (*18*) that the open−closed transition precedes the hydrolysis step but the assignment of rate constants differs slightly. They suggested that the simplest way to account for the requirement for a previously unobserved closing event would be to have a metastable closed M*·ATP state that broke down rapidly to either M†·ATP or M*·ADP·P$_i$. The evidence presented here shows, in contrast, that M*·ATP is a relatively stable species in rapid equilibrium with M†·ATP and in slower equilibrium with M*·ADP·P$_i$. We cannot rule out a scheme in which M*·ATP forms directly from M·ATP and M†·ATP is on a side branch because M†·ATP and M*·ATP are in rapid equilibrium. However, such a mechanism requires a more complicated scheme to explain the fluorescence quench seen on ADP binding.

Earlier studies on rabbit skeletal myosin fragments, prior to crystal structures, provided evidence for two interconvertible myosin conformers for each nucleotide state (*4, 30*). In particular, it was proposed that the AMP·PNP complex existed in two significantly populated states at 25 °C, although at lower temperatures one form predominated. The converse was observed with ADP, with only one form detectable at 25 °C but two forms at 5 °C. Trybus and Taylor (*4*) marginally favored a scheme in which the slow step was reversible and the rapid step was more irreversible. The temperature (Figure 3 and ref *23*) and pressure jump (Figure 4) data suggest the opposite could apply, although these techniques might be resolving further steps. Unambiguous comparison with the Dd W501+ construct is difficult because the equilibria may be poised slightly differently. We have no evidence for two significantly populated states for the ADP complex that are sensed by W501 in the Dd motor domain. Fluorescence measurements on skeletal myosin contain contributions from several tryptophan residues, so that some changes may reflect local events elsewhere in the molecule. This could explain the contrasting result with ADP. The absence of any pressure jump transients for W501+, in the absence of nucleotide or in the presence of saturating ADP, indicates that these states are predominantly in a single global conformation, although their fluorescence intensities and emission maxima show that they do not have identical structures (*13*). This result contrasts with previous temperature jump experiments on SH1-labeled skeletal myosin that revealed two conformations of the apo state which interconvert at 120 s^{-1} at 20 °C (*31*). Again, it would appear that
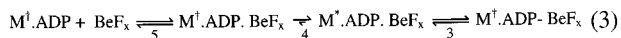
this result might reflect a local rather than a global conformational transition.

For the Dd motor domain examined here, the magnitude of the rate constant in the closed−open direction ($k_{-3a} \approx 800$ s^{-1} at 20 °C and ≈ 250 s^{-1} at 5 °C, Table 2) appears comparable to the binding isomerization rate constant, k_2 (>400 s^{-1} at 20 °C and 130 s^{-1} at 2 °C; Figure 2a and ref *13*), so that M†·ATP and M*·ATP remain close to equilibrium during their formation on rapid mixing. k_2 is difficult to determine for the W501+ construct because a transient is only resolved at low temperatures. However, incorporation of a tryptophan residue close to the nucleotide binding site (F129W or R131W constructs) gives an additional large fluorescence change that allows better definition of k_2, although much of the signal is still lost in the dead time of the stopped-flow apparatus (M. Kovács, A. Málnási-Csizmadia, and C. R. Bagshaw, unpublished observations). Nevertheless, from these constructs it is clear that k_2 is 1−2 orders of magnitude faster than the observed rate of hydrolysis ($K_{3a}k_{3b} + k_{-3b}$) across the 5−20 °C temperature range and thus k_2 and k_{-3a} are comparable throughout. It is also apparent that step 2 itself may be resolvable into substeps, particularly at low temperatures where reactions are better resolved. Corresponding steps in the presence of actin are currently being investigated, but rate constant data in the literature suggest that step 3a remains close to equilibrium during the ATP-induced dissociation ($k_{diss} = 400$ s^{-1}) of the actin−motor domain complex (*6*).

The mechanism of formation of the ADP·BeF$_x$ complex is more complicated because the BeF$_x$ moiety probably binds to the prebound ADP complex via the "back door" of the active site (*32*). Phosphate, and phosphate analogue, binding and release via the back door appear to require the open state because access is blocked (>95% occluded) in the closed state crystal structures. However, even in the open state, some breathing of the back door would be required for phosphate exchange. The BeF$_x$ (γ-phosphate group equivalent) appears about 70% occluded in the open crystal structures. Thus a simple two-state open−closed model is oversimplistic for the multiple conformations that myosin displays. Phosphate analogue binding follows saturation kinetics and has been analyzed in terms of a rapid and reversible weak binding step followed by a slow isomerization to trap the M·ADP·P$_i$ analogue state (*33−35*). For example, for AlF$_4^-$:

$$\text{M}^{\dagger}\text{.ADP} + \text{AlF}_4^- \underset{5}{\rightleftharpoons} \text{M}^{\dagger}\text{.ADP. AlF}_4^- \underset{4}{\rightleftharpoons} \text{M}^{*}\text{.ADP. AlF}_4^- \quad (2)$$

For the Dd W501+ construct, the rate constant for the fluorescence enhancement on addition of BeF$_x$ reaches a maximum of 0.15 s^{-1}, which may be assigned to k_{-4} and has an apparent K_5 value of 1 mM. The rapid transient (1000 s^{-1}) observed on perturbation of the M·ADP·BeF$_x$ state (Figures 3b and 4a) therefore requires an additional transition (step 3) of the trapped complex to give a second open state.

$$\text{M}^{\dagger}\text{.ADP} + \text{BeF}_x \underset{5}{\rightleftharpoons} \text{M}^{\dagger}\text{.ADP. BeF}_x \underset{4}{\rightleftharpoons} \text{M}^{*}\text{.ADP. BeF}_x \underset{3}{\rightleftharpoons} \text{M}^{\dagger}\text{.ADP- BeF}_x \quad (3)$$

There is ambiguity in the order of the later two states. It is possible that the closed−open transition (step 3) is associated with the formation of a covalent link between an ADP terminal oxygen atom and the beryllium atom, as has been implicated in the crystal structure (*14*) and NMR studies (*35*).

The latter investigation found that multiple ^{19}F signals were present in the M·ADP·BeF$_x$ complex, with an average Be:F ratio of 1.7−1.9, and thus the structure is not a simple adduct of ADP and BeF$_3$. Such a covalent M†·ADP−BeF$_x$ complex would account for it mimicking the M†·ATP state and hence the similarity in the kinetics of the open−closed transition as compared with ATP and AMP·PNP.

Equation 3 might suggest that the open−closed transition (i.e., switch 2 movement as sensed by W501) is not tightly coupled to the opening of the back door to allow BeF$_x$ binding and release; otherwise, the open M†·ADP−BeF$_x$ state, which represents at about 50% of the bound nucleotide at equilibrium, would allow rapid exchange of BeF$_x$. Alternatively, covalent bond formation may inhibit the loss of the BeF$_x$ from this complex. In the case of AlF$_4$, the maximum binding rate constant for the formation of the complex is about 50 times less than for BeF$_x$. In contrast to the ADP·BeF$_x$ complex, ADP·AlF$_4$ does not mimic the M†· ATP state. There is no indication of covalent bonding in the crystal structure (*14*), and the Al:F ratio remains close to 4 (*35*). No rapid transient is seen by pressure jump, indicating that the concentration of M†·ADP−AlF$_4$ is negligible, and hence eq 2 remains a satisfactory description. The deviation in the fluorescence signal from linearity at low temperatures might be related to multiple states that are in slow equilibrium (i.e., equivalent to step 4 in eq 2). Any reequilibration on the minutes time scale following pressure perturbation would be difficult to detect due to long-term drift in the signal.

Attempts to study P$_i$ binding to M†·ADP have been thwarted by its weak interaction, although ^{18}O isotope exchange and ^{32}P incorporation provide direct evidence for reversibility of steps 3−5 in eq 1 for skeletal myosin (*36*, *37*). To date there is no rigorous estimate of the value of K_4 in eq 1 because it is difficult to achieve saturation in P$_i$ incorporation experiments. It is normally assumed that $k_4 = 0.05$ s^{-1} and the K_4 equilibrium lies to the right in eq 1. However, it could be argued that the slow phosphate release rate is due to the predominance of the closed M*·ADP·P$_i$ state, which must first open to give an unfavorable M†·ADP· P$_i$ state prior to P$_i$ release; i.e., $K_4 \ll 1$ and $K_4k_5 = 0.05$ s^{-1}. This (partial) coupling between the open−closed transition and rate-limiting P$_i$ release through the back door provides a natural explanation for the effect of modification of the SH1 thiol in skeletal myosin (*38*). This modification favors more the open state (K_{3a} smaller and K_4 larger), as judged by the reduced enhancement of fluorescence in the steady state, and gives a reduced effective rate for hydrolysis ($K_{3a}k_{3b}$) but an overall increase in the steady-state basal turnover rate (K_4k_5).

Temperature and pressure jump perturbations have been applied to isolated thick filaments and muscle preparations with the intent of identifying cross-bridge states and their interconversion rates. In the case of isolated vertebrate thick filaments, it has been noted that increased temperature in the presence of ATP gives rise to an ordering of the cross-bridges along the filament backbone (*39*). Although this state was initially assumed to require ATP hydrolysis to give the vertebrate M**·ADP·P$_i$ state, the possibility was raised that ordering was more closely associated with the closed conformation (*40*). In the case of whole muscle, temperature jumps are associated with a rapid rise in tension (*41*). This finding was interpreted to result mainly by a shift from

nonstereospecifically bound cross-bridges to stereospecifically bound ones that exerted tension, rather than to an increase in the number attached because the stiffness remained constant. However, a shift from the open to closed conformation of the free heads would also tend to promote an increase in tension due to a potential increase in cross-bridge binding.

In isometrically contracting muscle fibers, an increase in pressure of 100 bar (10 MPa) results in a 10% fall in tension (*42*). Since a significant fraction of myosin heads are detached under all conditions (relaxed, shortening or isometric contraction), then application of increased pressure is expected, on the basis of the results presented here, to result in a reduction in the M*·ATP and M*ADP·P$_i$ closed states and increased occupancy of the M†·ATP open state. This could lead to loss of tension as the overall cycle responds to the changed steady-state concentrations. However, the rapid release of the applied pressure results in an increase in tension, and the rate of tension recovery is sensitive to the concentration of P$_i$ in the solution (*43*). This has been interpreted as compatible with the pressure-sensitive step being coupled to the release of P$_i$ from a preforce A−M·ADP·P$_i$ complex to form an A·M·ADP force holding state. If this transition were simply a reversal of the open−closed structural change, as seen in crystals of the isolated myosin motor, while attached to actin, then a decrease in volume would be expected and the force generating transition would be enhanced at high pressure. The fact that the opposite occurs is a clear indication that the force-generating event is not simply a reversal of open-to-closed structural change. To achieve the opposite volume change requires that any volume change accompanying the closed−open-like transition of the attached state is more than compensated for by volume changes occurring on P$_i$ release and at the actomyosin interface during this process. Previous solution studies have established the volume changes accompanying actin binding to vertebrate myosin subfragment 1 (or, more accurately, the volume change of an acto-subfragment 1 isomerization, +100 mL/mol; *44*), mantADP binding to subfragment 1 (+58 mL/mol; D. S. Pearson, G. Holtermann, and M. A. Geeves, unpublished observations), and ADP binding to acto-subfragment 1 (+59 mL/mol; *45*). In principle, each step of the cross-bridge cycle can have an associated volume change, and these should sum to the volume change of ATP hydrolysis as for any other thermodynamic parameter. As yet, data are insufficient to check the detailed balance.

In the course of this work full details of the temperature jump measurements of Urbanke and Wray (*46*) became available. These workers focused on tryptophan signals from vertebrate skeletal myosin subfragment 1, but because of the larger sample volume (3 mL) of their apparatus, they were able to record transient signals even in the presence of nonresponsive tryptophan residues. Overall, their data and conclusions are in good agreement with ours. As expected for skeletal myosin, the apparent rate constant for the hydrolysis step was slightly faster, and in the presence of ADP, the fluorescence was enhanced rather than quenched. They reported slightly less temperature dependence of the K_{3a} equilbrium constant than we found, but the small difference in the slopes of the steady-state fluorescence with temperature (Figure 1) is largely due to the contribution of the nonresponsive tryptophan residues in their protein samples. Nevertheless, the finding of a rapid transient prior to the hydrolysis step is similar to our findings and argues for a loose coupling between the nucleotide state and the conformational state [the down−up transition (*46*) is equivalent to open−closed transition in our terminology]. Urbanke and Wray (*46*) analyzed their data in terms of a general two-conformational-state parallel pathway, although their modeling showed that the data could be fit by essentially a linear scheme in which the major flux occurred via the equivalent of the M†·ATP ↔ M*·ATP ↔ M*·ADP·P$_i$ pathway. In conclusion, we demonstrate that fluorescence emission specifically from Dd W501, located in the relay loop, appears to monitor closely events at the opposite end on the relay helix and is thus sensitive to the open−closed transition of the switch 2 loop at the nucleotide binding site. The finding of a rapid transient change in fluorescence, following perturbation by temperature or pressure, demonstrates that this structural change is not tightly coupled to the hydrolysis step per se, although the latter step does bias the overall equilibrium in the case of hydrolyzable substrates such as ATP.

ACKNOWLEDGMENT

REFERENCES

1. Werber, M. M., Szent-Györgyi, A. G., and Fasman, G. D. (1972) *Biochemistry 11*, 2872−2883.
2. Bagshaw, C. R., Eccleston, J. F., Eckstein, F., Goody, R. S., Gutfreund, H., and Trentham, D. R. (1974) *Biochem. J. 141*, 351−364.
3. Johnson, K. A., and Taylor, E. W. (1978) *Biochemistry 17*, 3432−3442.
4. Trybus, K. M., and Taylor, E. W. (1982) *Biochemistry 21*, 1284−1294.
5. Millar, N. C., and Geeves, M. A. (1988) *Biochem. J. 249*, 735−743.
6. Kurzawa, S. E., Manstein, D. J., and Geeves, M. A. (1997) *Biochemistry 36*, 317−323.
7. Hiratsuka, T. (1992) *J. Biol. Chem. 267*, 14949−14954.
8. Park, S., Ajtai, K., and Burghardt, T. P. (1997) *Biochemistry 36*, 3368−3372.
9. Park, S., and Burghardt, T. P. (2000) *Biochemistry 39*, 11732−11741.
10. Batra, R., and Manstein, D. J. (1999) *Biol. Chem. 380*, 1017−1023.
11. Yengo, C. M., Chrin, L. R., Rovner, A. S., and Berger, C. L. (2000) *J. Biol. Chem. 275*, 25481−25487.
12. Onishi H., Konishi, K., Fujiwara, K., Hayakawa, K., Tanokura, M., Martinez, H. M., and Morales, M. F (2000) *Proc. Natl. Acad. Sci. U.S.A. 97*, 11203−11208.
13. Málnási-Csizmadia, A., Woolley, R. J., and Bagshaw, C. R. (2000) *Biochemistry 39*, 16135−16146.
14. Fisher, A. J., Smith, C. A., Thoden, J., Smith, R., Sutoh, K., Holden, H. M., and Rayment, I. (1995) *Biochemistry 34*, 8960−8972.
15. Smith, C. A., and Rayment, I. (1996) *Biochemistry 35*, 5404−5417.
16. Dominguez, R., Freyzon, Y., Trybus, K. M., and Cohen, C. (1998) *Cell 94*, 559−571.
17. Houdusse, A., Kalabokis, V. N., Himmel, D., Szent-Györgyi, A. G., and Cohen, C. (1999) *Cell 97*, 459−470.
18. Geeves, M. A., and Holmes, K. C. (1999) *Annu. Rev. Biochem. 68*, 687−728.
19. Bauer, C. B., Holden, H. M., Thoden, J. B., Smith, R., and Rayment, I. (2000) *J. Biol. Chem. 275*, 38494−38499.

20. Sasaki, N., Shimada, T., and Sutoh, K. (1998) *J. Biol. Chem. 273*, 20334−20340.

21. Suzuki, Y., Yasunaga, T., Ohkura, R., Wakabayashi, T., and Sutoh, K. (1998) *Nature 396*, 380−383.

22. Málnási-Csizmadia, A., Kovács, M., Woolley, R. J. Botchway, S. W., and Bagshaw, C. R. (2001) *J. Biol. Chem. 276*, 19483−19490.

23. Jahn, W., Urbanke, C., and Wray, J. (1999) *J. Anat. 194*, 601.

24. Gutfreund, H. (1995) *Kinetics for the Life Sciences*, Cambridge University Press, Cambridge.

25. Clegg, R. M., and Maxfield, B. W. (1976) *Rev. Sci. Instrum. 47*, 1383−1392.

26. Manstein, D. J., Schuster, H.-P., Morandini, P., and Hunt, D. (1995) *Gene 162*, 129−332.

27. Peterman, B. F. (1979) *Anal. Biochem. 93*, 442−444.

28. Shih, W. M., and Spudich, J. A. (2001) *J. Biol. Chem.* (in press).

29. Kliche, W., Fujita-Becker, S., Kollmar, M., Manstein, D. J., and Kull, F. J. (2001) *EMBO J. 20*, 40−46.

30. Shriver, J. W., and Sykes, B. D. (1981) *Biochemistry 20*, 2001−2012.

31. Lin, S.-H., and Cheung, H. C. (1992) *FEBS Lett. 304*, 184−186.

32. White, H. D., Cartwright, S., Bellnap, B., and Zhang, X.-Z. (2001) *Biophys. J. 80*, 79a.

33. Werber, M. M., Peyser, Y. M., and Muhlrad, A. (1992) *Biochemistry 31*, 7190−7197.

34. Phan, B., and Reisler, E. (1992) *Biochemistry 31*, 4787−4793.

35. Henry, G. D., Maruta, S., Ikebe, M., and Sykes, B. D. (1993) *Biochemistry 32*, 10451−10456.

36. Trentham, D. R., Eccleston, J. F., and Bagshaw, C. R. (1976) *Q. Rev. Biophys. 9*, 217−281.

37. Goody, R. S., Hofmann, W., and Mannherz, H. G. (1977) *Eur. J. Biochem. 78*, 317−324.

38. Sleep, J. A., Trybus, K. M., Johnson, K. A., and Taylor, E. W. (1981) *J. Muscle Res. Cell Motil. 2*, 373−399.

39. Wray, J. S. (1987) *J. Muscle Res. Cell Motil. 8*, 62.

40. Xu, S., Gu, J., Rhodes, T., Belknap, B., Rosenbaum, G., Offer, G., White, H., and Yu, L. C. (1999) *Biophys. J. 77*, 2665−2676.

41. Tsaturyan, A. K., Bershitsky, S. Y., Burns, R., and Ferenczi, M. A. (1999) *Biophys J. 77*, 354−372.

42. Fortune, N. S., Geeves, M. A., and Ranatunga, K. W. (1989) *J. Muscle Res. Cell Motil. 10*, 113−123.

43. Fortune, N. S., Geeves, M. A., and Ranatunga, K. W. (1991) *Proc. Natl. Acad. Sci. U.S.A. 88*, 7323−7327.

44. Coates, J. H., Criddle, A. H., and Geeves, M. A. (1985) *Biochem. J. 232*, 351−356.

45. McKillop, D. F. A., Geeves, M. A., and Balny, C. (1991) *Biochem. Biophys. Res. Commun. 188*, 552−557.

46. Urbanke, C., and Wray, J. (2001) *Biochem. J. 358*, 165−173.